

Preliminary Analysis of Continuous Seismic Monitoring at Utah FORGE: Tracking Fracture Evolution with Distributed Acoustic Sensing and Permanent Seismic Sources

Julia Correa¹, Jonathan Ajo-Franklin², Todd Wood¹, Barry Freifeld³, and the FOGMORE@FORGE team

¹Lawrence Berkeley National Laboratory, Energy Geosciences Division, Berkeley, CA, USA

²Rice University, Earth, Environmental and Planetary Sciences, Houston, TX, USA

³Class VI Solutions Inc., Oakland, CA, USA

juliacorrea@lbl.gov

Keywords: vertical seismic profiling (VSP), distributed acoustic sensing (DAS), timelapse seismic monitoring, FORGE, EGS

ABSTRACT

Downhole distributed acoustic sensing (DAS) and permanently installed surface orbital vibrators (SOVs) were used for monitoring subsurface changes during hydraulic stimulation at the Utah FORGE EGS research site, as part of the DOE funded FOGMORE project. SOVs generate highly repeatable compressional (P) and shear (S) waves, making them ideal for long-term subsurface imaging and monitoring. During the 2024 stimulation at Utah FORGE, we recorded continuous seismic data with DAS and recorded a series of interstage vertical seismic profile (VSP) gathers using autonomous permanent sources, SOVs. By monitoring the stimulation using VSP data acquired with SOV/DAS, we can detect scattering events from fractures, giving insights into fracture dynamics. In this study, we present preliminary results of the VSP data acquired in monitoring well 16B(78)-32. We installed SOVs at four locations and evaluated the quality of the acquired SOV/DAS VSP data. All SOV locations present a rich wavefield recorded on the VSP gathers, with SOV2 and SOV3 showing the highest signal-to-noise ratio. SOV2 location reveals existing structure within the granite body. Further analysis is needed to detect potential changes associated with hydraulic fracturing.

1. INTRODUCTION

Enhanced geothermal systems (EGS) rely on the creation of fracture networks to enable fluid circulation and heat exchange at depth. Understanding and monitoring the evolution of fracture networks in EGS projects is crucial to optimizing stimulation and ensuring long-term reservoir performance. In this context, the Utah Frontier Observatory for Research in Geothermal Energy (FORGE) plays an important role in the development and understanding of geothermal energy resource extraction, serving as a testbed for advancing geophysical monitoring technologies in high-temperature environments. The FORGE project is located approximately 260 km southwest from Salt Lake City, Utah, near Milford. The geothermal resources onsite originate from a crystalline granitoid body with temperatures of approximately 175°C and above, which is overlaid by Quaternary alluvial deposits (Knudsen et al., 2019).

The growth and prediction of hydraulic fractures is traditionally done through rock mechanics modeling and core measurements, as well as through geophysical methods such as imaging logs and microseismic monitoring (Maxwell, 2014; Birkholzer et al., 2021). More recently, fiber-optics sensing technologies have emerged as transformative tools for the observation and understanding of fracture evolution. Distributed acoustic sensing (DAS) is a fiber-optics sensing technology that can be used for seismic monitoring, offering advantages in comparison with conventional tools due to its high spatial and temporal resolution over long distances, as well as its ability to be deployed permanently for long-term applications (Hartog, 2017; Mateeva et al., 2017). Numerous studies have demonstrated the use of DAS for the detection of fractures induced by hydraulic stimulation, from detecting fracture hits (Jin and Roy, 2017) to the detection of microseismic events (Lellouch et al., 2020).

One geophysical method that has been relatively underutilized in this context is timelapse vertical seismic profiling (VSP). Studies, such as Willis et al. (1992) and Meadows and Winterstein (1994), have demonstrated that VSP can be used to detect hydraulic fractures. Furthermore, VSP data acquired with DAS can be a powerful tool to capture scattering energy from hydraulic fractures and determine fracture geometry, as demonstrated in Byerley et al. (2018) and Titov et al. (2022). Although these studies focus on hydraulic fracturing in unconventional reservoirs, they offer valuable insight into how to better characterize and monitor fracture evolution in EGS reservoirs.

Surface orbital vibrators (SOVs) are permanently installed seismic sources used in conjunction with DAS to facilitate the acquisition of timelapse VSP data (Correa et al., 2021). They are designed to be permanently installed, operated remotely and autonomously. Recently, DAS/SOV VSP data has been demonstrated to provide unique insights into complex fracture dynamics during hydraulic fracturing (Correa et al. 2024), revealing aseismic opening and relaxation during and after stimulation using hourly snapshots during 9 continuous days of monitoring. This unprecedented sampling rate can enable more effective characterization and management of geothermal reservoirs, which subsequently supports the optimization of stimulation strategies.

Building on the successful use of DAS/SOV in hydraulic fracturing monitoring, we extend their application to the context of EGS. In this study, we explore the application of continuous seismic acquisition and monitoring using DAS and SOVs at the Utah FORGE site during the April 2024 experiment, as part of the Fiber-Optic Geophysical Monitoring of Reservoir Evolution (FOGMORE) project. We focus on the preliminary evaluation of the timelapse DAS/SOV VSP data, provide qualitative and quantitative analysis, and assess the observed

seismic scattering during and after hydraulic stimulation of the granitoid body. We aim to demonstrate the potential of DAS/SOV VSP to capture fracture evolution, offering a novel approach for monitoring EGS reservoirs.

2. FIELD EXPERIMENT

The Utah FORGE site serves as a field-scale test bed dedicated to advancing research into EGS technologies. The current experiment focuses on the monitoring of the hydraulic fracturing of a deep injection borehole, 16A(78)-32, throughout its stimulation and subsequent production in well 16B(78)-32, located approximately 100 m above the lateral of the injection well. The FORGE site is home to an extensive seismic monitoring array, consisting of a permanent surface network, nodal seismic deployment, borehole geophones, and permanently installed fiber-optic cables (Niemz et al., 2024).

The FOGMORE fiber-optics system at Utah FORGE uses a fiber-optic cable cemented behind the casing of 16B well. The cable consists of a combination of standard single-mode fiber, multi-mode fiber, and engineered single-mode fiber designed to enhance optical backscattering to improve sensitivity to seismic waves (Constellation, Silixa Ltd.). The cable was designed to withstand high temperatures, however, significant decay in optical loss was observed after cable manufacturing, which ultimately compromised the overall quality of the seismic data. The Constellation fiber is connected to a Silixa Carina interrogator unit, where seismic data was recorded continuously with output sampling rate of 1 kHz and spatial sampling of 1 m. The continuous DAS data was used for low-frequency DAS (LFDAS), microseismic monitoring, and VSP with SOVs.

The SOVs function similarly to vibroseis sources by generating a sweep signal across a range of frequencies. They generate seismic energy by rotating eccentric weights in clockwise (CW) and counterclockwise (CCW) directions, inducing circularly polarized waves, which can then be converted into vertical and horizontal components by summing or subtracting each direction of rotation, respectively (Daley and Cox, et al. 2001). While the rotational sweep of SOVs is not phase controlled, the generated compressional (P) and shear (S) waves are highly repeatable, making them ideal for long-term subsurface imaging and monitoring.

A total of four SOV sources were installed, located along and near the length of 16B well (Figure 1). Each location was determined based on seismic forward modeling, which identified the optimum configuration to ensure direct P-wave transmission to the area of interest, near the toe of the wells, while staying within permitted land access. Each SOV location consists of a motor controller, a 10 ton-force and 15 ton-force motors mounted to a 6 m³ concrete pad, and a seismic digitizer with solar panels. The two motors are concurrently operated over a 150 second sweep, with the smaller motor sweeping up to 80 Hz, while the larger motor sweeps up to 50 Hz. To record the pilot sweep, a near-field 4.5 Hz 3-component geophone is installed beneath the concrete pad, 5m below the ground surface. After being recorded locally, the sweeps were then transferred to a server near 16B wellpad for pre-processing.

Continuous SOV operation commenced in March 2024, prior to hydraulic stimulation of 16A well on April 3. During stimulation, the SOVs operated interstage to avoid potential interference with microseismic data acquisition. SOV operations continued until May, resuming later for circulation test with some operational modifications due to issues with the equipment. Here, we focus on the continuous timelapse data acquired with DAS and SOVs during the hydraulic stimulation conducted in April.



Figure 1: FORGE Utah field site in Milford, Utah. Orange circles show the location of the SOV sources; the injector well 16A is outlined in black; Utah FORGE Research Site is outlined in blue. In the left bottom corner, the figure shows a photo of an SOV location after installation where two motors were installed on a concrete pad.

3. DATA PROCESSING AND ANALYSIS

We performed a series of data processing steps to generate shot gathers from the continuous seismic data recorded with DAS. The processing workflow is outlined in Table 1. The first step involves synchronizing the sweep start times with the DAS GPS time to ensure alignment of the recorded signals. Once the sweep intervals are identified within the DAS dataset, we apply deconvolution to remove the recorded pilot signal from the DAS data. Deconvolution is used to minimize correlation sidelobes resulting from an unbalanced frequency spectrum (Daley and Cox, 2001), in contrast to the more common sweep correlation in vibroseis data processing. Following deconvolution, we separate each vintage of 20 sweeps into stacks of 10 sweeps each in the CW and CCW directions to improve signal coherence and attenuate random noise.

As part of the noise attenuation process, a band-pass filter is applied to the data from frequencies of 5 Hz to 70 Hz to suppress unwanted low-frequency and high-frequency noise. A spatial median filter is applied to mitigate horizontal striping artifacts commonly observed in DAS data, often referred to as "common-mode noise". The gathers are then sorted in the receiver domain, and a second pass of the spatial median filter is applied with a shorter window to further attenuate random noise. The next step removes the downgoing P to enhance the visibility of upgoing reflections by flattening the P arrival and applying an additional pass of spatial median filter. The last step aims to attenuate the remaining strong downgoing reflection from the granite interface by applying an F-K filter.

Figure 2 shows a shot gather for SOV2 acquired on April 10, after applying the processing steps. The left-most gather shows the data after band-pass filter and common-mode noise removal. Note that downgoing P is visible, as well as strong up-going reflections. However, the data exhibits strong levels of noise. After random noise attenuation with the spatial median filter in the receiver domain, there is a significant reduction on the levels of noise. The gather in the right shows the data after removing the downgoing P. Note that the upgoing reflections become more visible.

Table 1: Data processing flow applied to VSP data acquired with SOV/DAS.

<i>Process</i>	<i>Parameters</i>
Sweep deconvolution	Frequency domain deconvolution. 10% water level.
Stacking	10-sweep stack in CW and CCW directions, separately.
Band pass filter	10 to 70 Hz.
2D Spatial median filter	1001 trace window.
2D Spatial median filter in the receiver domain	21 trace window.
Flattening direct P	-
2D Spatial median filter	501 trace window.
F-K filtering	Filtering velocity equivalent to downgoing reflection from granite interface. 20% taper.

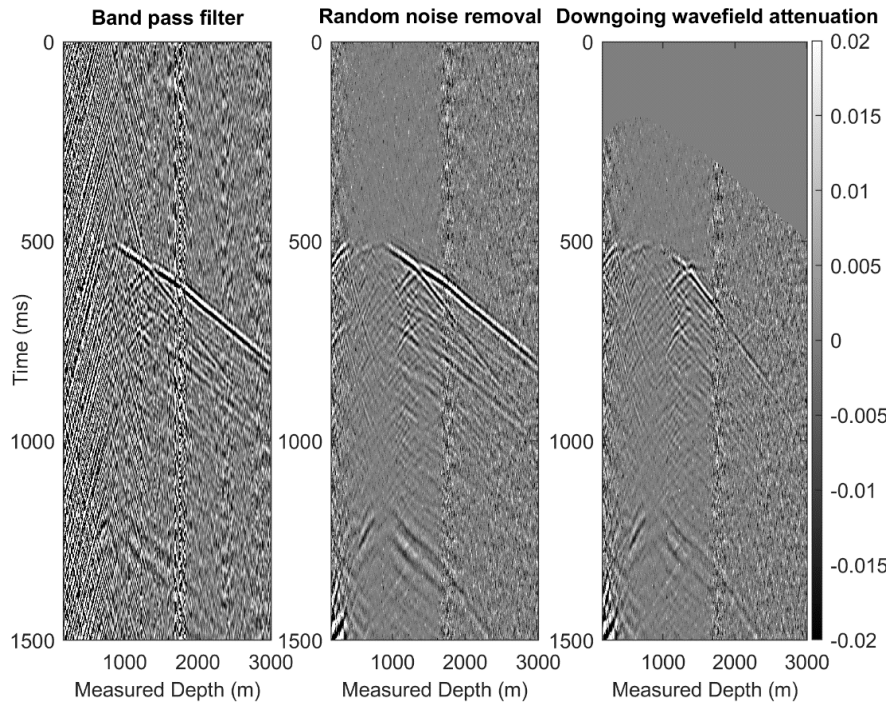


Figure 2: VSP shot gathers for SOV2 acquired on April 10, after data processing steps.

4. RESULTS

4.1 Shot Gathers

Figure 3 presents the processed VSP shot gathers for each SOV after applying stacking, band-pass filtering, and random noise attenuation (no wavefield separation). The gathers were acquired on April 10, with timestamps at 2:40:24 UTC for SOV1, 3:40:32 UTC for SOV2, 0:38:32 UTC for SOV3, and 17:39:54 UTC for SOV4. SOV1, SOV2, and SOV3 each consist of ten repeated sweeps stacked, and SOV4 has nine stacked sweeps.

The shot gathers reveal a complex wavefield, with clear downgoing P (blue arrows) and S (green arrows), along with upgoing reflections. Note that reflections from the granite-alluvial contact are consistently observed at all SOV locations (magenta arrows), attributed to the strong acoustic impedance contrast at this interface. Upgoing reflections from the granite interface seem to continue with time, suggesting the existence of a damage zone close to the interface. High noise levels are evident in the middle section of the fiber-optic cable (orange arrow), most likely due to the manufacturing defects mentioned previously, which degraded the overall quality of the VSP data, especially at greater depths.

Despite these limitations, reflections beyond the granite-alluvial interface are clearly observed, especially for SOV2 and SOV4 (black arrow), indicating that the DAS/SOV VSP data is able to detect structures within the granite body. Such reflections are one of the main components for further timelapse monitoring observations, as they can undergo changes associated with hydraulic stimulation. The ability to resolve such features highlights the potential of DAS and SOV data for continuous, high-resolution timelapse monitoring of fracture evolution in EGS reservoirs.

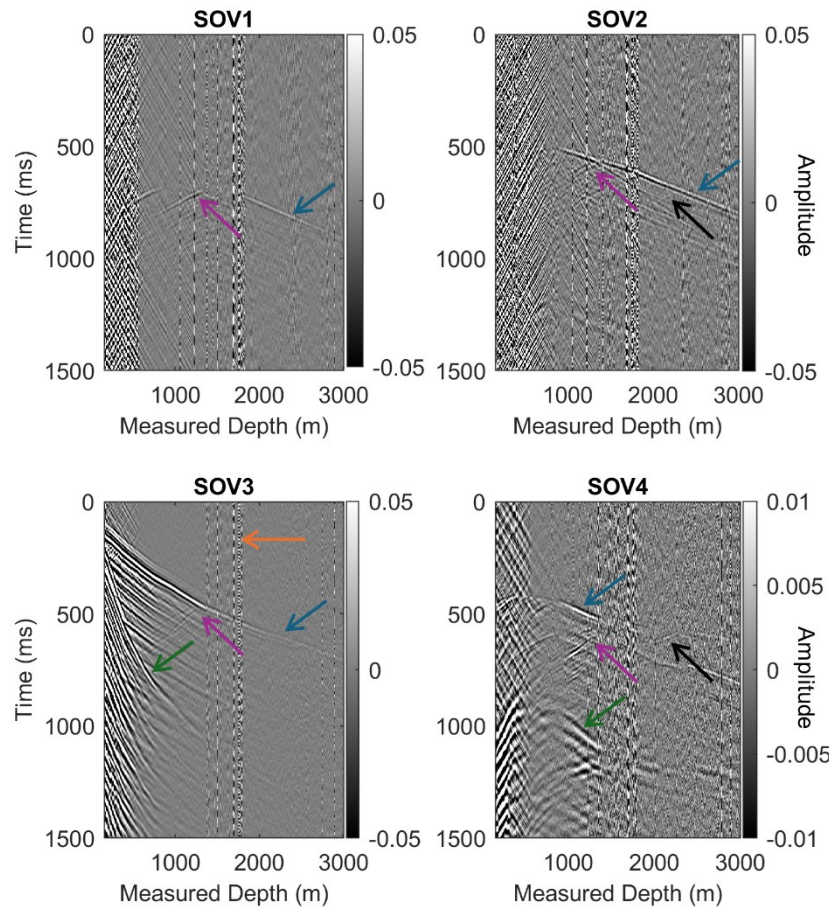


Figure 3: Examples of VSP shot gathers acquired with SOV/DAS for source locations SOV1, SOV2, SOV3 and SOV4 (stacked, reverse rotation) and recorded on 16B well. Shots have band pass filter and common-mode noise removal applied. The blue arrows indicate the direct P arrival, the green arrows indicate the direct S arrival, the magenta arrows point to a reflection from the granite/alluvial interface, and the orange arrow indicates noise on the fiber-optic cable most likely due to faulty manufacturing.

4.2 Quantitative Analysis of Data Quality

To further evaluate the quality of the VSP data acquired with DAS and SOVs, we analyzed the variations in signal-to-noise ratio (SNR) throughout the April stimulation period. The SNR was calculated for all SOV shot gathers after noise attenuation, before downgoing P removal. The SNR is calculated by taking the root-mean-square (RMS) amplitude within a 50 ms window around the first break, divided by the RMS amplitude of a noise window at the beginning of the record.

Figure 4 shows the SNR calculated for every shot gather during April, for each SOV location. SOV1 exhibits an SNR close to 0 dB, indicating that the signal and noise levels are nearly equivalent despite the applied noise attenuation techniques. A slight increase in SNR is observed beyond a measured depth of approximately 1800 m, attributed to improved coupling of the direct P-wave with the lateral section of the well. Given that SOV1 is the westernmost source location, the incident P-wave approaches the fiber axis at greater depths, leading to enhanced coupling and detection of the P wave.

SOV2 displays relatively high SNR levels, reaching approximately 20 dB. However, the SNR varies significantly across different sweeps, with fluctuations of up to 15 dB, likely due to elevated shut-in noise during certain phases of the experiment. Despite these variations, the lateral section of the well shows higher SNR, making this source particularly important for sensing signals from the stimulated region near the toe of the well.

SOV3, positioned closest to the 16B wellhead, demonstrates high SNR along the vertical portion of the well. This is expected, as the source location provides better coupling for the direct P-wave along the fiber cable. However, beyond a measured depth of approximately 1000 m, significant decline in SNR is observed. This reduction aligns with the location of the granite-alluvial interface, suggesting that the direct P-wave undergoes significant attenuation when entering the high impedance contrast of the granite-alluvial boundary. Along the lateral section of the well, SOV3 exhibits SNR values close to 0 dB, indicating significant noise contamination and reduced sensitivity.

SOV4 consistently exhibits the lowest SNR among all source locations. Unlike the other sources, which are positioned west of the 16B wellhead, SOV4 is located to the east, in the Mag Lee wash. This position seems to result in more attenuation of the wavefront in relation of the granite, leading to weaker transmitted P-wave energy and lower SNR across the dataset. Low Q sediment deposited in the wash

where SOV4 is located might explain the SNR difference. These observations underscore the importance of optimal source placement relative to well geometry and subsurface structure to maximize signal sensitivity in VSP acquisitions.

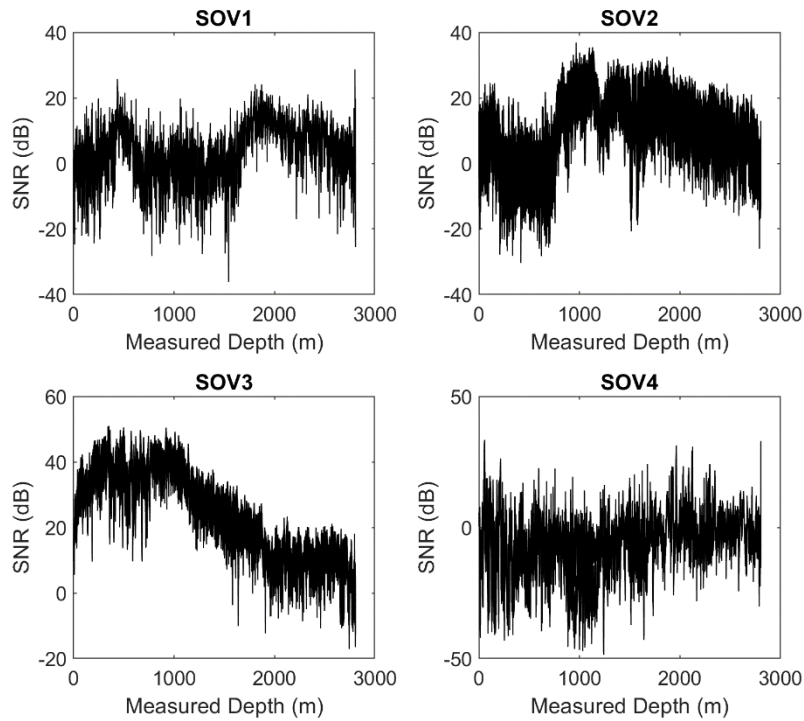


Figure 4: Signal to noise ratio of DAS VSP for sources SOV1, SOV2, SOV3 and SOV4 (reverse rotation) after data processing.

4.3 Preliminary Timelapse Analysis

We perform a preliminary investigation of the timelapse seismic data acquired by DAS and SOVs, focusing the analysis on the two source locations with the highest SNR, SOV2 and SOV3. The objective of this analysis is to identify sections exhibiting changes in the scattering signal over time, which could potentially indicate the formation of new fractures during stimulation or the development of existing fractures. The timelapse VSP data displayed in Figure 5 and Figure 6 are the shot gathers during April after applying FK filtering.

Figure 5 shows the data for SOV2. The first shot gather is the baseline, acquired March 28. The magenta arrow points to a strong reflection related to the granite interface. Note that the upgoing reflection exhibits a trail of subsequent reflections, potentially indicating a complex damage zone near the interface of the granite. A second reflection, highlighted by the blue arrow, appears within the granite body. Note that the reflection is present on the baseline data, suggesting it is scattered energy from an existing fault or fracture. The reflection persists over time; however, it appears to increase in length after approximately April 21st. Though, this needs further investigation to assess if the change in length is associated with an increase in height of the existing fracture. No other reflections are visible towards the toe of the well due to the high levels of noise. Figure 6 shows the timelapse data for SOV3 location. Strong reflections are observed at the interface of the granite; however, reflections within the granite are not clear in the timelapse signal, and especially difficult to identify due to the presence of high background noise.

Although the time-lapse analysis does not reveal obvious changes in the backscattered signal, the expected variations are relatively small compared to the overall amplitude of the recorded wavefield. To improve the detection of fracture-related changes in future analyses, additional noise attenuation techniques should be explored, and stacking of a larger number of repeated sweeps should be implemented to enhance signal coherence and reduce background noise.

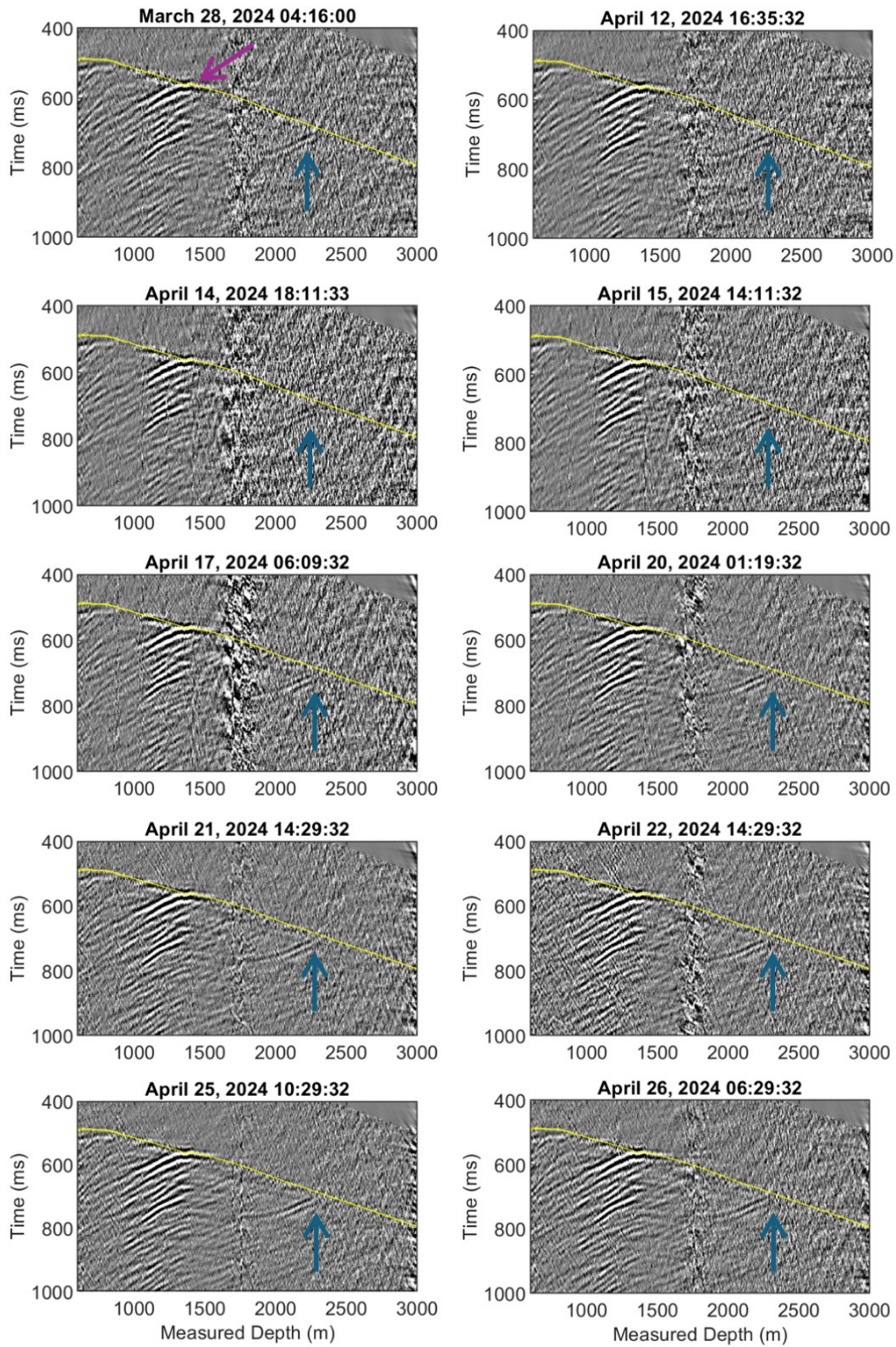


Figure 5: Timelapse VSP data acquired with DAS and SOV2 source during April stimulation. First break pick is displayed in yellow. Blue arrow indicates reflection within the granite body.

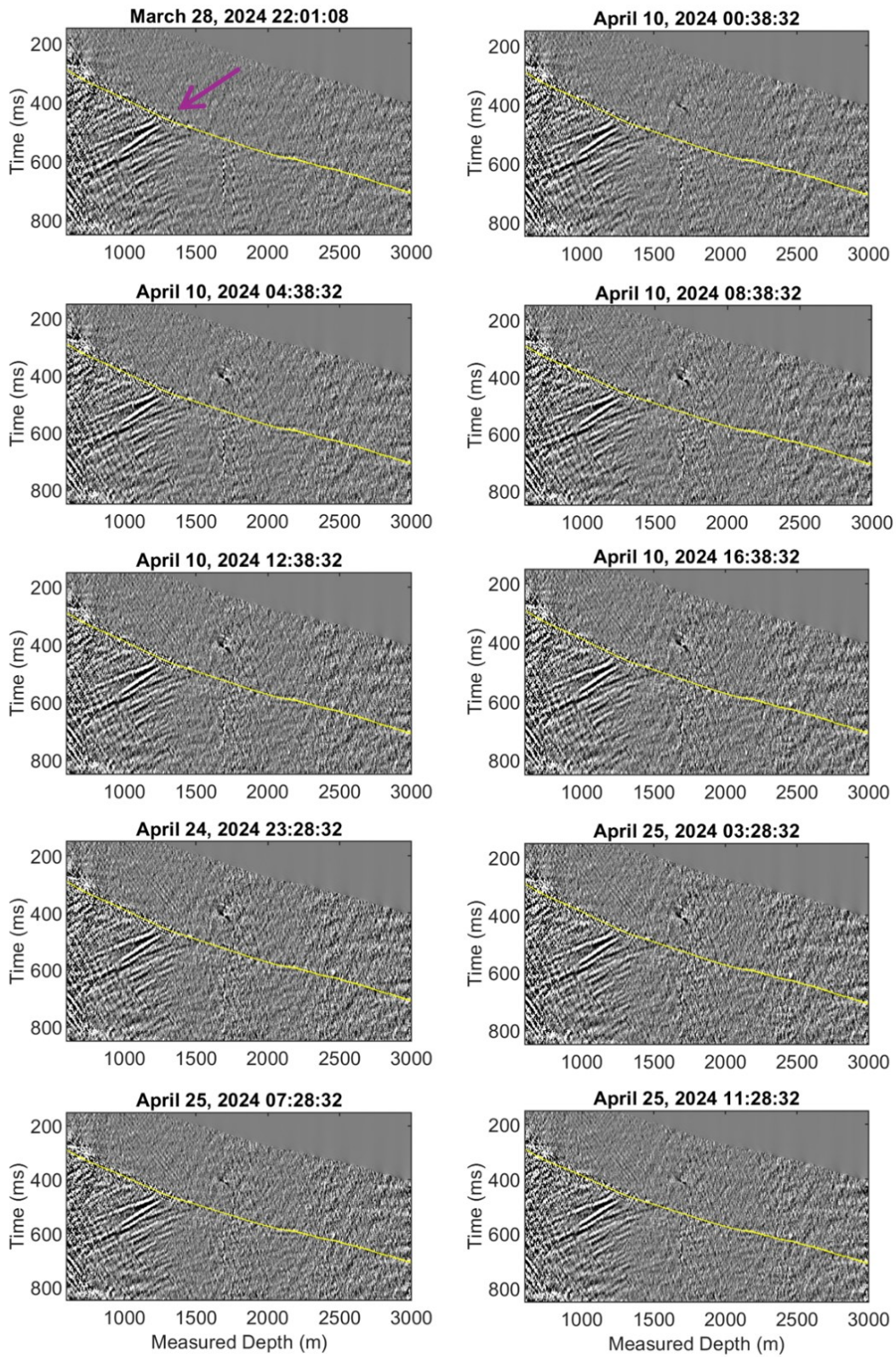


Figure 6: Timelapse VSP data acquired with DAS and SOV3 source during April stimulation. First break pick is displayed in yellow. Blue arrow indicates reflection within the granite body.

5. DISCUSSION AND CONCLUSIONS

Here, we present a novel method for the monitoring of fracture evolution at the FORGE Utah site based on fiber-optics sensing, DAS, and permanent seismic sources, SOVs. An engineered fiber-optic DAS cable (Constellation, Silixa) was used to acquire continuous seismic data in the producer well, 16B. However, after manufacturing, the cable showed signs of optical loss, which ultimately affected the signal quality. In this study we present a preliminary analysis of the timelapse VSP data acquired with DAS and SOV interstage hydraulic fracturing to understand fracture dynamics during the April 2024 stimulation of the 16A injection well. We also present a qualitative and quantitative analysis on the quality of the acquired dataset. We installed an array of four SOVs along and near the lateral of the well. The SOVs generate repeatable seismic energy that travel through the granite body. The aim is to monitor changes in the scattered seismic energy due to changes in the granite body, either through the creation of new fractures or the development of existing fractures. This method has the potential to revolutionize fracture monitoring at EGS sites by providing snapshots of the fracture evolution at high temporal sampling, and thus potentially enabling better characterization of geothermal reservoirs.

The timelapse VSP with DAS/SOV data acquired at each source location shows a rich wavefield consisting of downgoing P and S waves, as well as reflected waves. We observed reflections from the granite and alluvial interface, as well as reflections within the granite body. This result aligns well with microseismic cloud reported by Niemz et al. (2024), indicating the presence of existing faults and fractures in the granite during the April 2024 experiment. High levels of noise were also observed in the shot gathers, particularly after measured depth of approximately 1600 m, most likely due to defects in the manufacturing process previously identified in the installed fiber-optic cables.

SNR varied significantly across different source locations. SOV1 exhibits low SNR (~0 dB), with slight improvement beyond 1800 m due to better P-wave coupling along the lateral well section. SOV2 shows relatively high SNR, around 20 dB, with improved SNR near the toe of the well. SOV3 demonstrates high SNR along the vertical well due to its proximity to the wellhead but exhibits a significant decline beyond 1000 m, likely due to attenuation at the granite-alluvial interface. SOV4 consistently has the lowest SNR, possibly due to increased attenuation as the wavefront reaches the strong granite-alluvial interface. These observations highlight the role of source positioning relative to the well geometry and granite interface, which can play a role on the attenuation of the seismic signal and thus data quality.

We focus the preliminary time-lapse analysis on SOV2 and SOV3, as they showed the highest SNR. For SOV2, a strong reflection at the granite interface suggests a complex damage zone. We can also observe a strong reflection at around 2400 m measured depth within the granite body, which persists throughout April. The same reflection is seen in the baseline, meaning it is an existing structure that could potentially undergo further development during stimulation. SOV3 shows strong reflections at the granite interface, but no observed reflections within the granite body.

While no clear changes in backscattered signals are observed, scattering variations are expected to be small in relation to the amplitude of the full wavefield. Additionally, we were able to observe the existence of complex structures within the granite. Future work will focus on improving data quality through additional noise attenuation, and integrating additional datasets, such as microseismic data, to enhance the interpretability of the results. With further development, SOV/DAS technology offers a unique methodology to resolve, at high resolution, subtle subsurface changes associated with stimulation and production in EGS projects.

ACKNOWLEDGEMENTS

Funding provided by DOE EERE Geothermal Technologies Office to Utah FORGE and the University of Utah under Project DE-EE0007080 Enhanced Geothermal System Concept Testing and Development at the Milford City, Utah Frontier Observatory for Research in Geothermal Energy (Utah FORGE) site. Lawrence Berkeley National Laboratory authors provide research under Contract No. DE-AC02-05CH11231 with the U.S. Department of Energy.

REFERENCES

- Birkholzer, J. T., Morris, J., Bargar, J. R., Brondolo, F., Cihan, A., Crandall, D., Deng, H., Fan, W., Fu, W., Fu, P., and Hakala, A.: A new modeling framework for multi-scale simulation of hydraulic fracturing and production from unconventional reservoirs, *Energies*, 14, (2021), 641, doi: 10.3390/en14030641.
- Byerley, G., D. Monk, P. Aaron, and M. Yates: Time-lapse seismic monitoring of individual hydraulic frac stages using a downhole das array: *The Leading Edge*, 37, (2018), 802–810, doi: 10.1190/tle37110802.1.
- Correa, J., Isaenkov, R., Yavuz, S., Yurikov, A., Tertyshnikov, K., Wood, T., Freifeld, B. M., and Pevzner, R.: DAS/SOV: Rotary seismic sources with fiber-optic sensing facilitates autonomous permanent reservoir monitoring, *Geophysics*, 86, (2021), P61–P68, doi: 10.1190/geo2020-0612.1.
- Correa, J., Glubokovskikh, S., Nayak, A., Luo, L., Wood, T., Zhu, X., Ajo-Franklin, J., and Freifeld, B.: Revealing complex subsurface dynamics with continuous seismic monitoring: Observations using distributed acoustic sensing and surface orbital vibrators during hydraulic fracturing, *Geophysics*, 89, (2024), P47–P56, doi: <https://doi.org/10.1190/geo2023-0785.1>.
- Daley, T. M., and Cox, D.: Orbital vibrator seismic source for simultaneous P- and S-wave crosswell acquisition, *Geophysics*, 66, (2001), 1471–1480, doi: 10.1190/1.1487092.
- Hartog, A. H.: *An Introduction to Distributed Optical Fibre Sensors*, CRC Press (Taylor and Francis) (2017).

Correa et al.

- Jin, G., and Roy, B.: Hydraulic-fracture geometry characterization using low-frequency DAS signal, *The Leading Edge*, 36, (2017), 975–980, doi: 10.1190/tle36120975.1.
- Knudsen, T., Kleber, E., Hiscock, A., and Kirby, S. M.: Quaternary geology of the Utah FORGE site and vicinity, Millard and Beaver Counties, Utah, in *Geothermal characteristics of the Roosevelt Hot Springs System and Adjacent FORGE-EGS Site*, in Allis, R., and Moore, J. N., Utah Geological Survey Miscellaneous Publication: 169-B, (2019), B1–B29, doi: <https://doi.org/10.34191/MP-169-B>.
- Lellouch, A., Lindsey, N. J., Ellsworth, W. L., and Biondi, B. L.: Comparison between distributed acoustic sensing and geophones: Downhole microseismic monitoring of the FORGE geothermal experiment, *Seismological Society of America*, 91, (2020), 3256–3268, doi: 10.1785/0220200149.
- Mateeva, A., Lopez, J., Chalenski, D., Tatanova, M., Zwartjes, P., Yang, Z., Bakku, S., de Vos, K., and Potters, H.: 4D DAS VSP as a tool for frequent seismic monitoring in deep water, *The Leading Edge*, 36, (2017), 995–1000, doi: 10.1190/tle36120995.1.
- Maxwell, S.: Microseismic imaging of hydraulic fracturing: Improved engineering of unconventional shale reservoirs, SEG (2014).
- Meadows, M., and Winterstein, D.: Seismic detection of a hydraulic fracture from shear-wave VSP data at Lost Hills field, California, *Geophysics*, 59, (1994), 11–26, doi: 10.1190/1.1443523.
- Niemz, P., McLennan, J., Pankow, K. L., Rutledge, J., and England, K.: Circulation experiments at Utah FORGE: Near-surface seismic monitoring reveals fracture growth after shut-in, *Geothermics*, 119, (2024), 102947.
- Titov, A., G. Jin, G. Binder, and A. Tura: Distributed acoustic sensing time-lapse vertical seismic profiling during zipper-fracturing operations: Observations, modeling, and interpretation: *Geophysics*, 87, (2022), no. 6, B329–B336, doi: 10.1190/geo2021-0758.1.
- Wills, P. B., DeMartini, D. C., Vinegar, H. J., Shlyapobersky, J., Deeg, W. F., Woerpel, J. C., Fix, J. E., Sorrells, G. G., and Adair, R. G.: Active and passive imaging of hydraulic fractures, *The Leading Edge*, 11, (1992), 15–22, doi: 10.1190/1.1436884.